

PAPER DETAILS

TITLE: Modeling and optimization of a superstrate solar cell based on $\text{Cu}_2\text{ZnSn}(\text{S}_x\text{Se}_{1-x})_4/\text{ZnS}$ structure

AUTHORS: Abdelkader Aissat, Hahet Arbouz, Jean Pierre Vilcot

PAGES: 65-74

ORIGINAL PDF URL: <https://dergipark.org.tr/tr/download/article-file/360359>

Modeling and optimization of a superstrate solar cell based on $\text{Cu}_2\text{ZnSn}(\text{S}_x\text{Se}_{1-x})_4/\text{ZnS}$ structure

Abdelkader Aissat

LATSI Laboratory, Faculty of Technology, University of Blida 1, BP270, 09.000, Blida, Algeria,
arbouzhayet@yahoo.fr, orcid.org/ 0000-0003-3635-8568

Hahet Arbouz

LATSI Laboratory, Faculty of Technology, University of Blida 1, BP270, 09.000, Blida, Algeria,
arbouzhayet@yahoo.fr, orcid.org/0000-0003-2780-5215

Jean Pierre Vilcot

Institut d'Electronique, de Microélectronique et de Nanotechnologie, UMR CNRS 8520, Université des Sciences et Technologies de Lille1, Avenue Poincaré, CS 60069, 59652 Villeneuve d'Ascq, France,
jean-pierre.vilcot@iemn.univ-lille1.fr, orcid.org/0000-0002-6448-4740

Arrived: 28.08.2017 Accepted: 06.11.2017 Published: 08.11.2017

Abstract: The Kestrite semiconductor material $\text{Cu}_2\text{ZnSnSe}_4$ (CZTSe) is believed to be a suitable candidate for replacing the $\text{CuIn}_{1-x}\text{Ga}_x\text{Se}_2$ (CIGS) absorber for the abundance and the non-toxicity of its components. However, the record efficiency of solar cells based on this material reaches 11% which is lower than the conversion efficiency of the CIGS based solar cell for which the efficiency has reached 25%. The aim of this study is to model and optimize the electrical performances of a superstrate type solar cell based on the kestrite material $\text{Cu}_2\text{ZnSn}(\text{S}_x\text{Se}_{1-x})_4$ (CZTSSe). The goal is to investigate the effect of mixing the sulfide (S) component with selenide (Se) on the conversion efficiency η , band gap E_g open circuit voltage V_{oc} , short circuit current density J_{sc} , fill factor FF and maximum power density P of the device, through the evaluation of their behavior as a function of the ratio $S/(S+Se)$, which represents the concentration of sulfur in the absorber material CZTSSe. It is also shown in this work, through the calculation of the mismatch strain ϵ at the interface between the absorber and the buffer layers, that the zinc sulfide (ZnS) is a more appropriate buffer than cadmium sulfide (CdS) for the CZTSSe absorber. The effect of strain at the interface buffer/absorber on the bandgap energy of CZTSSe and then on the cell performances is evaluated. This evaluation is based on the strain theory in order to obtain more realistic results close to experimental results. It is noted that adding 72% of Sulfur in the absorber material, meaning that $x=0.72$, increases the efficiency to 13.1% therefore an improvement of 21.3% is obtained compared to the efficiency of the CZTSe solar cell with a strain equal to 0 meaning no deformation, $J_{sc}=15.35\text{mA}/\text{cm}^2$, $V_{oc}=0.800\text{V}$, $FF=74.1\%$ and $P_{max}=9.45\text{mW}/\text{cm}^2$.

Keywords: Thin film, semiconductor, CZTS, CZTSe Kestrites, solar cells,

Cite this paper: A. Aissat, H. Arbouz, , P. J. Vilcot, Modeling and optimization of a superstrate solar cell based on $\text{Cu}_2\text{ZnSn}(\text{S}_x\text{Se}_{1-x})_4/\text{ZnS}$ structure. Journal of Energy Systems 2017; 1(2): 65-74 DOI: 10.30521/jes.349137

© 2017 Published by JES peer-review scientific journal at DergiPark (www.dergipark.gov.tr/jes)

Nomenclature			
ZnS	Zinc Sulfide	CZTS	$\text{Cu}_2\text{ZnSnS}_4$
E_g	Band Gap	CZTSe	$\text{Cu}_2\text{ZnSnSe}_4$
J_{sc}	Short Circuit Current Density	CZTSSe	$\text{Cu}_2\text{ZnSn}(\text{S}_x\text{Se}_{1-x})_4$
Se	Selenide	S	Sulfur
CdTe	Cadmium Telluride	TCO	Transparent Conductive Oxide
CIGS	Copper Indium Gallium Selenide	V_{oc}	Open Circuit Voltage
In	Indium	J_{ph}	Photo generated Current Density
Ga	Gallium	FF	Fill Factor
Cd	Cadmium	η	Efficiency

1. INTRODUCTION

During the last decade, photovoltaic technology has known a real development in particular the technology of thin films [1]. Several research works have been devoted to solar cells based on cadmium telluride (CdTe) and copper indium gallium selenide (CIGS) which have achieved conversion efficiencies of 22.1% and 22.6% [2] respectively while efficiency for an 841-cm² CIGS module fabricated by Solar Frontier was substantially boosted to 19.2% [3].

However, because of difficulties with the supply of indium (In), which is rare metal and gallium (Ga) in addition to their high cost, and the toxicity of cadmium (Cd), it will be important to replace these elements by others, which are abundant in the crust of the Earth, inexpensive and non-toxic to reduce the environmental damage. On the other hand, the challenge currently faced by the future generation of thin film solar cells is to improve efficiency while reducing the cost of manufacturing.

In this context, Cu₂ZnSnS₄ (CZTS), Cu₂ZnSnSe₄ (CZTSe) and their alloys Cu₂ZnSn(S_xSe_{1-x})₄ (CZTSSe) of I₂-II-IV-VI₄ group are considered to be good substitutes for CIGS thin film because of the similarity of their structures, their excellent properties such as a large light absorption surpassing 10⁴cm⁻¹ in visible wavelength region for application of solar cell [4,5], optimal direct band gap and the abundance and non-toxicity of all their constituents. The interest focused on this type of materials is increasing continuously, important efforts are centered on research, and development of CZTS, CZTSe and CZTSSe based solar cells, which have become some of the most attractive research projects in recent years. The conversion efficiency of CZTS based solar cells has been improved from 0.66% [6] to the current certified record of 12.6% in 2013 [7] with a 13.8% small-area device reported in 2016 [8]. Several methods of deposition vacuum or not have been experimented for the fabrication of CZTS, CZTSe and CZTSSe thin film absorbers, highly efficient CZTSSe based solar cells have been fabricated by thermal evaporation [9] and reactive sputtering process [10]. Despite the progress achieved in this area of research, the conversion efficiency of devices based on kestrite materials is not competitive with that of CIGS based solar cells. Several causes cited in the literature are at the origin of this low efficiency, such as secondary phase in the bulk and non-favorable alignment of the conduction band at the interface between the CZTSSe absorber and the CdS buffer [11, 12]. In addition, the most important is high defects density in the material as well as small grain size, which cause short diffusion length carriers [13]. Improving efficiency require a good understanding of the influence of basic factors on the cell performances.

The purpose of our study is to model and optimize the structure of a superstrate solar cell based on the absorber material CZTSSe. The manufacture of a superstrate type solar cell begins by the deposition of the transparent conductive oxide (TCO) layer on a transparent substrate, then a buffer layer type-n followed by an absorbent layer type-p and finally, a metallic electrode layer is deposited on the top of the absorber [14]. The fabrication of superstrate configuration solar cells has the advantage of low cost and simplifies the step of encapsulation necessary to protect the cells [15-17].

The cells made in superstrate configuration are typically made with an absorber layer of CdTe that contains cadmium known for its high toxicity. For this reason, it is better to replace the CdTe by a material that does not contain this element. The absorber material used in the present work is CZTSSe where sulfur element was introduced in the composition of the alloy. It was reported that one of the important ways to vary the properties of the absorber material is to introduce a mix of anions in the alloy. The addition of sulfur (S) to the selenide anion (Se) in the material absorber gives the ability to tune the energy band gap from 1 to 1.5 eV by varying the ratio $x = S/(S+Se)$ from 0 to 1. In this simulation the CdS usually used in the structure of the solar cell of substrate-type was replaced by ZnS buffer which is not polluting and which is more absorbent due to its higher band gap. Besides ZnS adheres better than CdS to the CZTSSe material and generates therefore a less significant deformation at the interface between the two layers. In this work the effect of the increase of the ratio x on mismatch strain at the interface between the layers of ZnS and CZTSSe as well as on their band alignment and consequently on the electric performance such as: open circuit voltage V_{oc} , photo generated current density J_{ph} , fill factor FF and efficiency η were investigated. The results obtained will allow understanding the behavior of a cell based on the heterojunction CZTSSe/ZnS in superstrate configuration and optimize the composition of sulfur in the absorber in order to achieve the best efficiency and optimal performance at optimal band gap.

2. THEORETICAL MODEL

The structure of a solar cell based on the heterojunction CZTSSe/ZnS base in superstrate configuration is represented in figure 1. The absorption coefficients of the absorber and the buffer layers are calculated using the model of Tauc as follows [18].

$$\alpha(E) = \alpha_0 \frac{\sqrt{E - E_g(x)}}{E} \quad E \geq E_g \quad (1)$$

Where α_0 is a constant and E is the photon energy.

The variation of the band gap energy of the CZTSSe as a function of sulfur concentration increase x in the absorber alloy is described in the following equation [19]

$$E_g(x) = x.E_{g(CZTS)} + (1-x)E_{g(CZTSe)} - bx(1-x) \quad (2)$$

Where b is bowing parameter which equals 0.08 for CZTSSe material.

In the simulation of the density of defects is considered to be affected by sulfur augmentation in the absorber alloy as:

$$N_t(x) = x.N_{t(CZTS)} + (1-x)N_{t(CZTSe)} \quad (3)$$

Where N_t is the defect concentration.

The total photo- generated current density $J_{ph}(\lambda)$ is the sum of photo- generated currents J_n (electron current density of the front region), J_p (hole current density of the base region) and J_w (current density in the depletion region) [19].

$$J_{ph}(\lambda) = J_n(\lambda) + J_p(\lambda) + J_w(\lambda) \quad (4)$$

The total photocurrent density is calculated on the whole range of the solar spectrum as [21]:

$$J_{ph} = \int_{\lambda_{min}}^{\lambda_{max}} q.EQE(\lambda).F(\lambda)d\lambda \quad (5)$$

Where $\lambda_{min}, \lambda_{max}$ are the minimum wavelength and maximum wavelength of the solar spectrum respectively.

$F(\lambda)$ is the incident photon flux. $EQE(\lambda)$ is the external quantum efficiency [22].

$$EQE(\lambda) = \frac{J_{ph}(\lambda)}{q F(\lambda)} \quad (6)$$

Where q is the electron charge.

The current voltage $J(V)$ characteristic of the solar cell is described by [13]

$$J(V) = J_{ph} - J_s \left(\exp\left(\frac{qV}{nKT}\right) - 1 \right) \quad (7)$$

Where K is Boltzman constant, T is the temperature, V is the voltage and n is the ideality factor.

$$J_s = J_{00} \cdot e^{\frac{E_g}{nKT}} \quad (8)$$

Where J_s is the saturation current [20] and J_{00} is a factor which depends on temperature.

Open circuit voltage is expressed as [24]:

$$V_{oc} = \frac{E_g}{q} - \frac{nkT}{q} \ln\left(\frac{J_{00}}{J_{ph}}\right) \quad (9)$$

The fill factor and the conversion efficiency are respectively [25]:

$$FF = \frac{J_{max} \cdot V_{max}}{J_{sc} \cdot V_{oc}} \quad (10)$$

$$\eta = \frac{J_{max} \cdot V_{max}}{P_i} \quad (11)$$

Where J_{max} , V_{max} are the maximal current density and maximum voltage of solar cell.

The band gap of the strained absorber layer is calculated on the base of the strain theory [16], it is necessary to know the mismatch strain, which has the following components in the case of, oriented (z-axis) growth [17].

$$\varepsilon = \varepsilon_{xx} = \varepsilon_{yy} = \frac{a_0 - a_b}{a_b}, \varepsilon_{zz} = -\frac{C_{12}}{C_{11}} (\varepsilon_{xx} + \varepsilon_{yy}) \quad (12)$$

Where ε_{xx} , ε_{yy} are the in-plane biaxial strain along the x and y directions and ε_{zz} is the out-of-plane strain along the growth z-direction.

Where a_b is the lattice parameter of the buffer layer and C_{11} , C_{12} are the elastic constants and a_0 is the lattice constant of the absorber which varies as function of x following the expression underneath:

$$a_0 = x \cdot a_{CZTS} + (1 - x) \cdot a_{CZTSe} \quad (13)$$

The conduction band E_c of the CZTSSe absorber is shifted by the following energy:

$$\delta E_c = a_c (\varepsilon_{xx} + \varepsilon_{yy} + \varepsilon_{zz}) \quad (14)$$

While the light hole and heavy hole valence bands are shifted by:

$$\delta E_{lh} = a_v (\varepsilon_{xx} + \varepsilon_{yy} + \varepsilon_{zz}) - \frac{b_s}{2} (\varepsilon_{xx} + \varepsilon_{yy} - 2\varepsilon_{zz}) \quad (15)$$

$$\delta E_{hh} = a_v (\varepsilon_{xx} + \varepsilon_{yy} + \varepsilon_{zz}) + \frac{b_s}{2} (\varepsilon_{xx} + \varepsilon_{yy} - 2\varepsilon_{zz}) \quad (16)$$

Where a_c , a_v are the hydrostatic potential deformations of conduction and valence bands respectively and b_s is the valence band shear deformation potential.

If the heavy hole sub band is upper than the light hole one that means the CZTSSe layer has a compressive strain. In this case, the strained band gap is expressed as:

$$E_{gst}(x) = E_g(x) + \delta E_c - \delta E_{hh} \quad (17)$$

However, if the light hole sub band is upper the CZTSSe layer has an extensive strain and the strained band gap is given by:

$$E_{gst}(x) = E_g(x) + \delta E_c - \delta E_{lh} \quad (18)$$

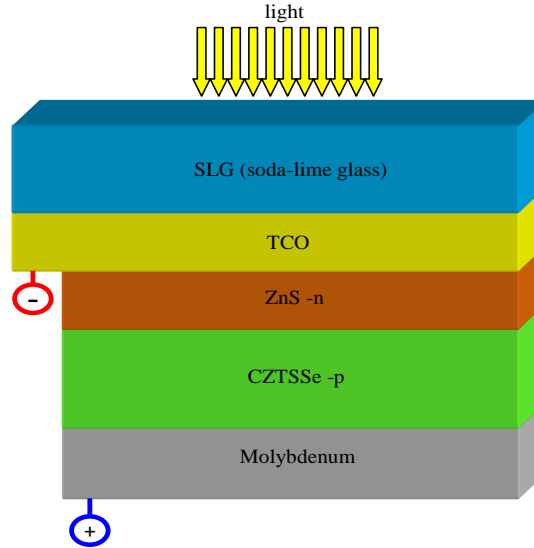


Figure 1. Simplified scheme, of a solar cell based on the hetero- junction CZTSSe/ZnS with a superstrate configuration.

3. RESULTS and DISCUSSION

Figure 2 represents the mismatch strain at the epitaxial absorber/buffer interface due to their difference of lattice constants of two different heterojunctions: CdS/CZTSSe and ZnS/CZTSSe as a function of the sulfur concentration x . Concerning the CZTSSe/CdS heterojunction, the value of the strain decreases from -5% up to -7.7% during the change in the concentration of sulfur from 0 which corresponds to the material CZTSe (pure selenium) up to 1 which corresponds to the material (pure sulfur) CZTS. It is noticed that the strain is always negative indicating that the CZTSSe absorber is tensile strained. In addition, the values are very high which indicates that the lattice misfit between the CdS and the CZTSSe is important. While the CdS is replaced by ZnS buffer, a match is obtained between the buffer and the absorber at $x = 0.72$ for which the strain equals 0. And if x varies from 0 to 0.72 the strain diminishes from 3.7% to 0% where the CZTSSe is compressively strained.

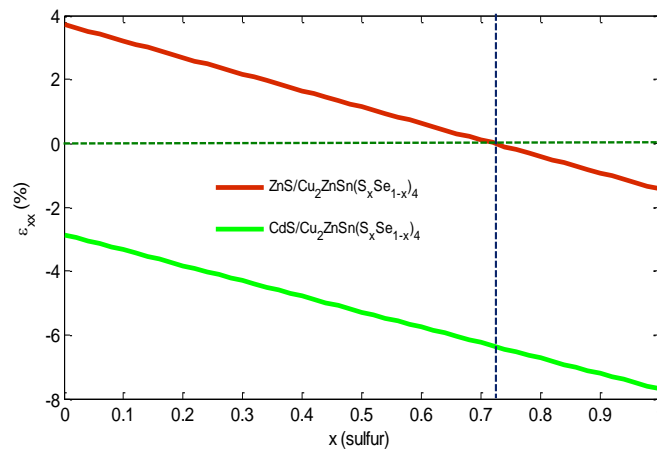


Figure 2. Variation of the mismatch strain as a function of concentration of sulfur. For CdS/ CZTSSe and ZnS/ CZTSSe based structures respectively

However, when x varies from 0.72 to 1 the strain falls down to -1.4% and on this range the CZTSSe layer is tensile strained. From this analysis, it is concluded that ZnS corresponds more and gives a better match with the CZTSSe absorber than CdS. In addition, it offers a better opportunity to minimize the deformation at the ZnS/CZTSSe interface by choosing an appropriate concentration of sulfur. In addition, when the buffer is made of CdS in a superstrate CZTSSe solar cell, a diffusion of cadmium into the absorber layer is observed but there is no diffusion of zinc or sulfur in the case of a buffer made of ZnS. However, ZnS deposited by chemical bath deposition contains defects, which are liable to

diffuse into the absorber [15]. This problem is overcome by using different methods of fabrication compared to those usually used for a substrate solar cell based on CZTSSe. The variation of the strained absorber band gap energy as sulfur concentration increases is represented in figure 3 and compared with its variation when the strain effect is neglected. The band gap energy concerning the unstrained case changes following the expression (2) from 1.02 to 1.51 eV. While when the effect of strain on bandgap is taken into account, two ranges of concentrations must be discussed: the first one is the range of 0 to 0.72 which concerns the case of compressive strain, the gap on this range is lower than that of the unstrained CZTSSe and varies from 0.94 to 1.39 eV. The second is the range of 0.72 to 1 where the strain is extensive and the bandgap is higher than that of the unstrained absorber and varies from 1.39 to 1.66 eV.

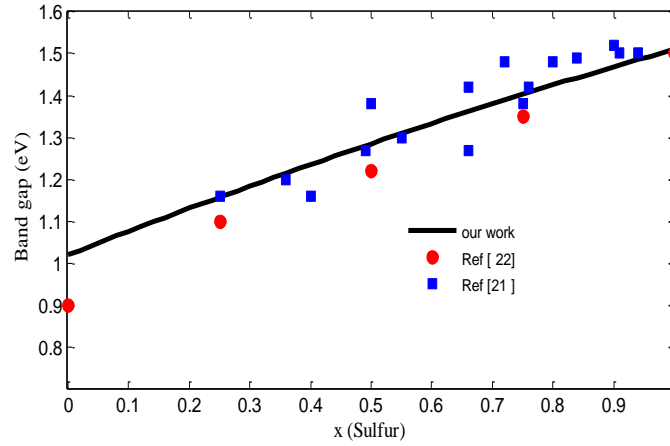


Figure 3. CZTSSe band gap energy as a function of concentration sulfur. For the structure based on unstrained ZnS/CZTSSe hetero-junction and for the structure based on strained ZnS/CZTSSe hetero-junction.

The experimental results of [22] are also represented in figure 3. The offset between experimental and simulated results varies from 0.01 to 0.07 eV when the strain is compressive and from 0 to 0.02 eV when the structure is extensively strained. It is noted that there is a discrepancy above the concentration 0.93 where the offset reaches 0.18 eV. Concerning [21], a good correlation of experimental and simulated results is observed below 0.7 of concentration with an offset varying between 0 and 0.05 eV where the strain is compressive. However above 0.75 of concentration the results begin to diverge and a maximum offset of 0.18 eV at $x=1$ is noted. The variation of the band gap has a direct influence on the coefficient of absorption, i.e. in the case where the strain is compressive, and where the gap is lower compared to that of the unstrained absorber, the absorption becomes more advantageous. However, when the strain becomes extensive where the band gap is higher the material becomes less absorbant. See figure 4. Figure 5(a) shows the variation of V_{oc} versus x of strained and unstrained absorber respectively. In the case where the effect of strain is neglected, the increase of V_{oc} when the sulfur concentration increases in the absorber CZTSSe material, from 0.623 to 0.858 V is noted. V_{oc} of the strained structure increases as well, but according to the previous variation of strained absorber band gap, V_{oc} is lower compared to that of unstrained structure, varying from 0.59 to 0.80 V on the range of 0 to 0.72 of x , where the strain is compressive and higher, varying from 0.800 V to 0.924 V between 0.72 to 1 of sulfur concentration where the strain is extensive. Compared to the experimental results of [22] depicted also in figure 5(a). There is a good correlation with simulation results when the structure is compressively strained where the offset between experimental and simulated values varies from 16 to 92 mV except for $x=0.5$ where the offset reaches 230 mV. Within the range of concentrations where the strain is extensive, a good correlation is noted between $x=0.74$ and $x=0.78$, however a divergence is noted above 0.8 of concentration where the offset reaches 202 mV.

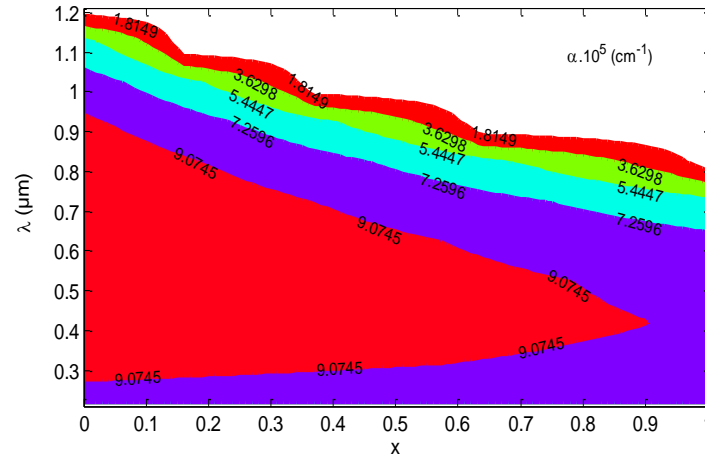


Figure 4. Absorption coefficient as a function of wavelength and the concentration of Sulfur

Figure 5(b) illustrates the variation of J_{sc} as x variation from 0 to 1. Concerning unstrained structure, a total loss of 17.34% is noted from 17.73 to 14.65 mA / cm². However, when the effect of strain is considered, a loss of short current density of 17.91% from 18.1 to 15.35 mA / cm² is noted on the range of 0 to 0.72. A higher loss of 25.51% is noted up to 0.72 from 15.35 to 12.23 mA/cm². In addition, J_{sc} is higher than that of unstrained CZTSSe on the first range and becomes lower in the second. Figure 5 (c.) represents efficiency as a function of x for the two structures mentioned above. For the unstrained one the efficiency increases as the increase of the concentration of sulfur from 0 to 1 in the CZTSSe absorber material from 11.1% to 13.5% which corresponds to a total increase of 21.62%. But concerning the strained structure an increase of efficiency from 10.8% to 13.1% is noted below 0.72 of concentration where the strain is compressive then starts to decrease below 0.72 down to 12.3%.

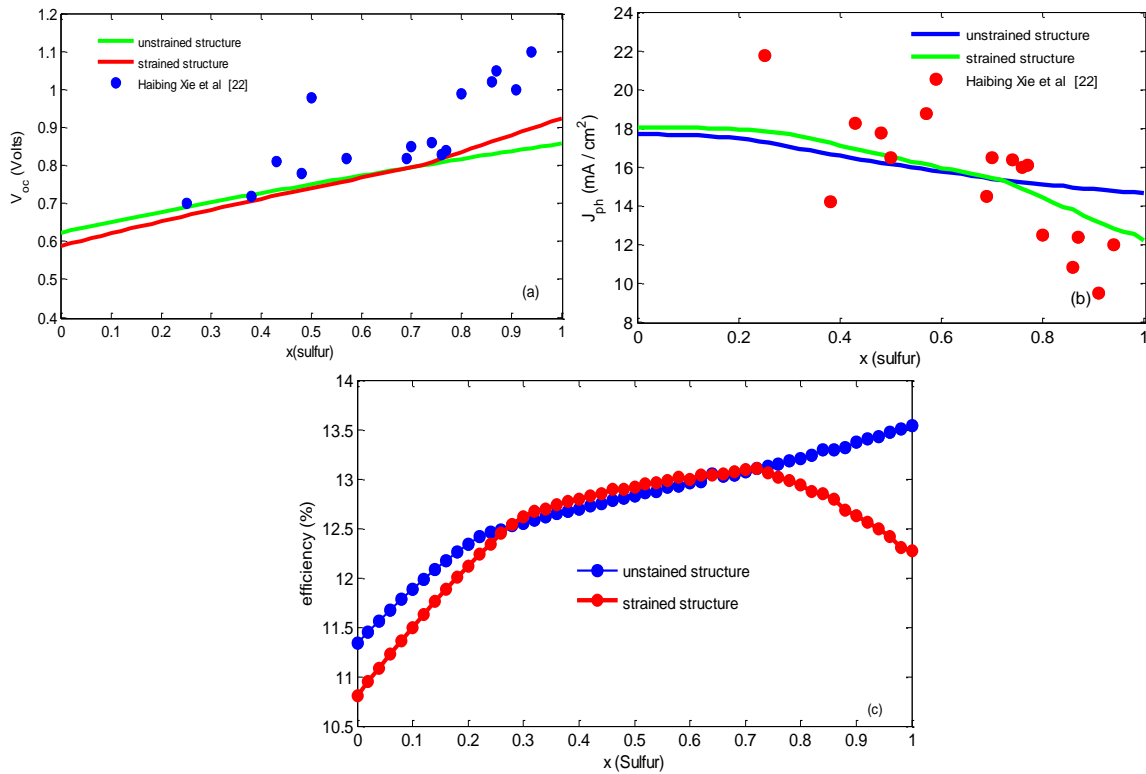


Figure 5. (a) Open circuit voltage V_{oc} versus concentration of sulfur x for unstrained and strained ZnS/CZTSSe structures respectively (b) Short circuit density of current J_{sc} versus concentration of sulfur x for unstrained and strained ZnS/CZTSSe structures respectively and (c) Conversion efficiency η versus sulfur concentration x for unstrained and strained ZnS/CZTSSe structures respectively.

It is also noticed from the figure that on the range of 0.28 to 0.72 of concentration the efficiency of compressively strained CZTSSe structure is more advantageous than that noted for the unstrained one because of the better absorption on this range. When the effect of strain on device performance is considered, the maximum conversion efficiency of about 13% is obtained on the range of sulfur concentration varying from 0.56 to 0.72, which corresponds to a compressive strain varying from 0.8 to 0%.

Figure 6 depicts the characteristics J-V for different values of concentrations $x=0.3$ and $x=0.5$ belong to the range where the strain is of the compressive type however $x=0.9$ and $x=1$ belong to the range where the strain is extensive.

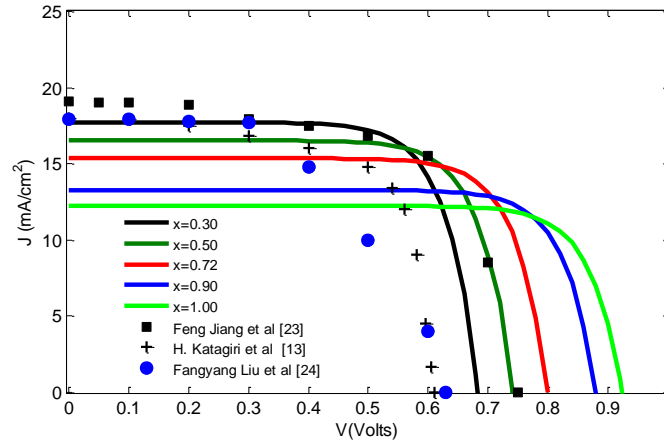


Figure 6. J-V characteristics for different values of concentrations: $x=0.3$ and $x=0.5$ belonging to the range where the strain is of the compressive type, $x=0.9$ and $x=1$ belong to the range where the strain is extensive and $x=0.72$ which corresponds to the perfect match between the buffer ZnS and the absorber CZTSSe.

The concentration $x=0.72$ corresponds to the perfect match between the buffer material ZnS and the absorber material CZTSSe. Compared to the experimental results given by [23] there is a good correlation between them and simulated results for $x=0.5$ where the offset of V_{oc} is 0V, and that of J_{sc} is about 1.6 mA/cm². However, the experimental results of [13] are close to the simulated curve for $x=0.3$ where the offset of V_{oc} is 0.06 V, and that of J_{sc} is about 0.01 mA/cm². The experimental curve [24] of CZTSSe based structure at $x=0.68$ is compared with the simulated curve at $x=0.72$ which have the closer concentration of sulfur, 2.3 mA/cm² and 0.17 V offsets of J_{sc} and V_{oc} were noted respectively. The P-V characteristic is represented in figure 7. It is shown that the maximum power density increases below $x=0.72$ when the strain is compressive but decreases above when the strain becomes extensive.

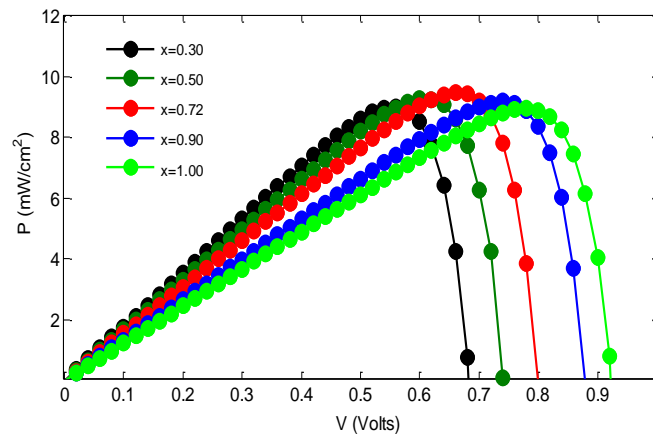


Figure7. P-V characteristics for different values of concentrations: $x=0.3$ and $x=0.5$ which correspond to compressively strained ZnS/CZTSSe structure $x=0.9$ and $x=1$ which correspond to tensile strained ZnS/CZTSSe structure. $x=0.72$ corresponds to the perfect match between the buffer ZnS and the absorber CZTSSe.

A maximum of 9.45 mW/cm^2 is noted at 0.72 where the strain equals 0. The simulation results are summarized in the following Table 1. It is possible to optimize the concentration of sulfur of the absorber material of the superstrate structure based on strained CZTSSe /ZnS heterojunction. The maximum of 13.1% of efficiency is obtained at the concentration of sulfur of 0.72 where the strain equals 0, $E_g=1.39\text{eV}$ which matches the maximum of light spectrum, $V_{oc}= 0.8\text{V}$, $J_{sc}=15.35\text{mA/cm}^2$ and $P = 9.45\text{mW/cm}^2$. Compared to the structure based on CZTSe (pure Selenium)/ZnS a gain of 2.3% of efficiency is noted with an increase of 211.3 mV of V_{oc} , 1.8 mW/cm^2 of maximum power density and 2.7 mA/cm^2 loss of J_{sc}

Table 1. Results of the simulation

x(Sulfur)	$E_g(\text{eV})$	$V_{oc}(\text{V})$	$J_{sc}(\text{mA/cm}^2)$	FF(%)	$\epsilon_{xx}(\%)$	P(mW/cm ²)	$\eta(\%)$
0	1.02	0.632	17.73	71.29	-3.4	8.04	11.33
0.68	1.37	0.791	15.47	74.04	0	9.40	13.04
0.80	1.41	0.817	15.11	74.36	0.7	9.55	13.21
0.86	1.46	0.830	14.95	74.51	1.0	9.60	13.30
1	1.51	0.858	14.65	74.83	1.7	9.81	13.53

4. CONCLUSION

In this paper, a simulation of superstrate solar cell based on CZTSSe/ZnS was performed. It was demonstrated that ZnS is a more appropriate buffer layer than CdS for the CZTSSe absorber layer since it has the ability to adjust the strain at the ZnS/CZTSSe interface by varying the concentration of Sulfur in the absorber material. The match between ZnS and CZTSSe occurs for 72% of sulfur in the CZTSSe alloy. It was also demonstrated that the mixture of Sulfur with Selenium in the CZTSe material has contributed to vary the electrical device performances. The effect of strain at the interface between the absorber material CZTSSe and ZnS buffer on the band gap energy of the absorber layer and then on the device performance has been investigated as a function of sulfur concentration variation. It has been reported that for $x=0.72$ which corresponds to a perfect match between buffer and absorber layers where it has been noticed an efficiency of 13.1% with a value of 15.35 mA/cm^2 of short current density, 0.800V of open circuit voltage, FF of 74.1%, maximum power density of 9.45mW/cm^2 and no strain. The obtained results are close to the experimental results reported at close concentration of sulfur. In addition, at this concentration value the band gap equals 1.4eV which corresponds to the maximum of sunlight spectrum. The obtained efficiency is better than that noted for ZnS/ (pure CZTSe) structure compared to which 21.30%, 35.82%, 5.12% and 5% improvements in efficiency, V_{oc} , FF and maximum power density have been realized respectively, however 17.91% loss of J_{sc} has been observed.

REFERENCES

- [1] Alshal, M.A. &Allam, N.K. Broadband Absorption Enhancement in Thin Film Solar Cells Using Asymmetric Double-Sided Pyramid Gratings, *J. Electrical Material*, 2016; 45: 5685–5694. <https://doi.org/10.1007/s11664-016-4735-7>
- [2] Green, M.A., Emery, K., Hishikawa, Y., *et al*, Solar cell efficiency tables (version 49), *Prog. Photovolt. Res. Appl.*, 2017; 25:3–13.
- [3] Green, M.A., Emery, K., Hishikawa, Y., *et al.*, Solar cell efficiency tables (version 50), *Prog. Photovolt. Res. Appl.*, 2017; 25(7): 668–676. <https://doi.org/10.1002/pip.2909>.
- [4] Walsh, A., Chen, S., Wei, S.-H., Gong, X.-G., Kesterite Thin-Film Solar Cells: Advances in Materials Modelling of $\text{Cu}_2\text{ZnSnS}_4$, *Adv. Energy Mater.*, 2012; 2(4): 400–409. <https://doi.org/10.1002/aenm.201100630>.
- [5] Khoshsir, N., Yunus, N.A.M., Numerical analysis of In_2S_3 layer thickness, band gap and doping density for effective performance of a CIGS solar cell using SCAPS, *J. Electronic Mat.*, 2016; 45(11): 5721–5727. <https://doi.org/10.1007/s11664-016-4744-6>.
- [6] Katagiri, H., Sasaguchi, N., Hando, S., *et al.*, Preparation and evaluation of $\text{Cu}_2\text{ZnSnS}_4$ thin films by sulfurization of e-b evaporated precursors, *Solar Energy Mater. Solar Cells*, 1997; 49(1–4): 407–414.
- [7] Wang, W., Winkler, M.T., Gunawan, O., *et al.*, Device characterization of CZTSSe thin-film solar cells with 12.6% efficiency, *Adv. Energy Mater.*, 2014; 4, 1301465.
- [8] Reported at PVSEC-36 by a research team led at DGIST in South Korea. A 0.181 cm^2 solar cell was certified at 13.80% by KIER.
- [9] Wang, K., Shin, B., Reuter, K.B., *et al.*, Structural and elemental characterization of high efficiency $\text{Cu}_2\text{ZnSnS}_4$ solar cells, *Appl. Phys. Lett.*, 2011; 98(5): 051912. <http://dx.doi.org/10.1063/1.3543621>

- [10] Li, J.B., Chawla, V., Clemens, B.M., Investigating the role of grain boundaries in CZTS and CZTSSe thin film solar cells with scanning probe microscopy, *Advanced Materials*, 2012; 24(6): 720-723.
- [11] Ericson, T., Scragg, J.J., Hultqvist, A., Zn(O, S) buffer layers and thickness variations of CdS buffer for $\text{Cu}_2\text{ZnSnS}_4$ solar cells, *IEEE J. Photovoltaics*, 2014; 4(1): 465-469.
- [12] Bodnar, I.V., Telesh, E.V., Gurieva, G., et al., Transmittance spectra of $\text{Cu}_2\text{ZnSnS}_4$ thin films, *J. Electronic Mat.*, 2015; 44(10): 3283–3287. <https://doi.org/10.1007/s11664-015-3909-z>
- [13] Katagiri, H., Jimbo, K., Yamada, S., Kamimura, T., et al., Enhanced conversion efficiencies of $\text{Cu}_2\text{ZnSnS}_4$ based thin film solar cells by using preferential etching technique, *Japan Society Appl. Phys.*, 2008; 014201.
- [14] Zeman, M., Thin-film silicon pv technology, *J. Electrical Engineering*, 61(5); 2010: 271–276.
- [15] Grenet, L., Altamura, G., Kohen, D., Fillon, R., et al., Process for producing a p-n junction in a CZTS-based photovoltaic cell and CZTS-based superstrate photovoltaic cell, 2013; *WO 2015015367 A1*.
- [16] Van de Walle, C.G., Band lineups and deformation potentials in the model-solid theory, *Phys. Rev. B*, 1989; 39:1871-1883.
- [17] Zhang, Y., Ning, Y., Zhang, L., Zhang, J., et al., Design and comparison of GaAs, GaAsP and InGaAlAs quantum-well active regions for 808-nm VCSELs, *Optics Express*, 2011; 19(13): 12569-12581.
- [18] Kosyachenko, A., Mathew, X., Paulson, P.D., Lytvynenko, V.Ya., Maslyanchuk, O.L., *Solar Energy Mater. Solar Cells* 2014; 130: 291–302.
- [19] Benmir, A., Aida, M.S., Analytical Modeling and Simulation of CIGS Solar Cells, *Energy Procedia*, 2013; 36: 618-627. <https://doi.org/10.1016/j.egypro.2013.07.071>
- [20] Charles J. Hages, James. Moore, Sourabh Dongaonkar, Muhammad. Alam, Mark Lundstrom, and Rakesh. Agrawal, Photovoltaic Specialists conference (PVSC), 38th IEEE 2012; pp 2658-2663.
- [21] Shiyu Chen, Aron Walsh, Ji-Hui Yang, X. G. Gong, Lin Sun, Ping-Xiong Yang, Jun-Hao Chu, and Su-Huai Wei, Compositional, *Physical Review B* 83, 2011; 125201.
- [22] Haibing Xie, Mirjana Dimitrievska, Xavier Fontané, Yudania Sánchez, Simon López-Marino, Víctor Izquierdo-Roca, Verónica, Bermúdez, Alejandro Pérez-Rodríguez, Edgardo Saucedo, baseds, *Solar Energy, Materials & Solar Cells*, 140, 2015; 289–298
- [23] Feng Jiang, Shigeru Ikeda, Zeguo Tang, Takashi Minemoto, Wilman Septina, Takashi Harada and Michio Matsumura, *Prog. photovolt. Res. Appl.* 23, 2015; 1884–1895.
- [24] Fangyang Liu, Fangqin Zeng, Ning Song, Liangxing Jiang, Zili Han, Zhenghua Su, Chang Yan, Xiaoming Wen, Xiaojing Hao and Yexiang Liu, *ACS Appl. Mater. Interfaces*, 2015; 7: 14376–14383